Physics Letters A 408 (2021) 127487

Contents lists available at ScienceDirect

Physics Letters A

www.elsevier.com/locate/pla

DFT study of silicene on metal (Al, Ag, Au) substrates of various thicknesses

Alexander Y. Galashev [a,b,*], Alexey S. Vorob'ev [a]

[a] Institute of High-Temperature Electrochemistry, Ural Branch of Russian Academy of Sciences, Academicheskaya Str., 20, Yekaterinburg 620990, Russia
[b] Ural Federal University named after the first President of Russia B.N. Yeltsin, Mira Str., 19, Yekaterinburg 620002, Russia

ARTICLE INFO

Article history:
Received 15 February 2021
Received in revised form 14 May 2021
Accepted 1 June 2021
Available online 4 June 2021
Communicated by L.M. Woods

Keywords:
Density functional theory
Molecular dynamics modeling
Silicene
Metal substrates

ABSTRACT

The silicene obtained on silver and gold substrates is not a subject for a large-scale use due to the high cost of the substrate materials. The aim of this work is to find a suitable low-cost substrate for the bulk production of silicene. In this work, three materials were investigated as a silicene substrate: Al, Ag, and Au. In all these cases, a metallic type of electronic conductivity was established in the silicene/substrate system. It turned out that the aluminum substrate provides an even better adhesion to silicene than the gold one. Silicene on the Al (111) substrate demonstrates the most uniform distribution of normal stresses with a minimum value of local bursts. Thus, aluminum seems to be quite a competitive material for the silicene production. The main obstacle in using aluminum substrates for the silicene production is strong oxidation in air.

1. Introduction

By cleaving 3D layered materials such as graphite, it is easy to obtain thin 2D materials such as graphene [1]. Layered 3D MoS_2 also splits well into the layers [2]. The presence of van der Waals interaction in the interlayer space is the reason for the easy production of thin films of graphite, as well as dichalcodenides, chlorides, thiophosphates, black phosphorus and black arsenic by exfoliation [3,4]. Recently, new 2D materials (graphite and transition metal) have been proposed. They can be effectively used as anode materials to improve battery performance and for other applications such as electronics [5,6].

As a rule, this method can be used to obtain 2D flakes with a characteristic size from tens to hundreds of microns [7]. These dimensions are insufficient for modern electronics. To perform the peeling, the surface must be well-adherent to the outer layer of the 3D laminate. Metal substrates provide sufficient adhesion to the surfaces of 3D laminates. Gold is distinguished among the metals used for this purpose, due to an exceptionally even and un-oxidized outer surface, which provides good adhesion to the layered material. The gold–assisted separation of layers makes it possible to obtain the thinnest films with a characteristic lateral size of up to 1 cm, i.e. at least 2 orders of magnitude greater than with any other metals used for exfoliation [4]. However, it is currently unknown if gold functions as a good exfoliation material for materials other than dichalcogenides, chlorides, thiophosphates, black phosphorus, black arsenic, and graphite. The behavior of gold and silver in contact with SiO_2 is thoroughly studied. Both gold and silver do not adhere very well to SiO_2. Noble metals Au and Ag do not form intermetallic oxide layers. Therefore, they are weakly bonded with SiO_2 as it is described by the van der Waals interaction [8]. Aluminum demonstrates a better adherence to SiO_2 than to gold or silver. Therefore, it is of interest to include in this study the system "silicene on a thin cut of aluminum" along with silicene contacting with Au and Ag. The adsorption of Al on silicene was studied using DFT calculations in [9]. It turned out that dense two-sided adsorption leads to an unstable configuration. This is due to the rather strong repulsive interaction between neighboring Al ad-atoms. The Al–Si bond lengths depend on the adsorption conditions and lengthen as the Al concentration increases.

In this work, we investigate the ability of various thin metals (Au, Ag, Al) slices to peel off a silicon monolayer, i.e. silicene. The structure of silicene is similar to that of graphene, but there is also a fundamental difference between them. The atoms of both structures are ordered in the honeycomb lattice. This structure contributes to the convergence of the physical properties of graphene and silicene [10,11]. However, sp^2 hybridization makes graphene absolutely flat, while mixing sp^2 and sp^3 hybridizations in silicene creates a buckling, the two-level silicene structure. Silicene is more stable when 'buckled' [12], i.e. when two sublattices are present in it, they are displaced relative to each other and form conditionally two planes. Due to the tendency of silicene to sp^3 hybridization,

* Corresponding author.
E-mail address: alexander-galashev@yandex.ru (A.Y. Galashev).

https://doi.org/10.1016/j.physleta.2021.127487
0375-9601/

the epitaxy is most likely process of the film formation, however, the possibility of other processes implied cannot be eliminated. To date, silicene has been obtained on various substrates (Ag, Au, Ir, graphite, MoS_2, sapphire, ZrB_2) [13–19]. With a sufficiently strong binding of silicene to the substrate surface, it can lose its remarkable electronic properties, in particular, the Dirac cone [20]. The substrate plays a very important role in maintaining the properties, which were found in freestanding silicene [21–23]. Questions related to the retention of the electronic properties of silicene, including the Dirac cone, on metal substrates were discussed in [20,24–27]. However, the change in the structure of the substrate itself after the silicene formation has not been considered, and the calculation of the stresses appearing in silicene has not been carried out.

In order to retain the attractive properties of silicene, it is preferable to obtain it on a semiconducting surface or on an insulating surface. In this case, the weakness of the interaction between the surface and silicene contributes to the preservation of the linear character of the band structure. However, difficulties arise in obtaining a 2D Si layer due to the appearance of a highly probable clustering of silicon atoms. In addition, the structure of silicene obtained on such surfaces turns out to be highly inhomogeneous. Therefore, for the silicene fabrication and use, it is important to investigate the adhesion properties of suitable metal substrates.

2. Model

We performed calculations using the Siesta software package [28]. Different silicene supercells were selected depending on the type of substrate. The silicene sheet was parallel to the xy plane and contained 18 atoms. To simulate it, 3 × 3 supercells were used. The silicene structure was represented by two sublattices (lower and upper) separated from each other by a distance of 0.044 nm. The layer of the metal substrate was specified as a 4 × 4 supercell consisting of 16 metal atoms. The substrate thickness varied from 1 to 5 layers. This was sufficient to determine the optimal number of layers (i.e. limiting their number) when performing accurate calculations. In addition, we have performed an approximate simulation of silicene formation on a sufficiently thick substrate. In this case, an increase in the thickness of the substrate was achieved by adding one more lower metal layer, which atoms could not move in the direction of the 0z axis, but moved in the *xy* plane. Therefore, this layer is considered as fixed.

The periodic (Born-von Karman) boundary conditions promoted the "expansion" of the system by representing a physical quantity in a Fourier series, using the set of all plane waves that satisfy the boundary condition. The combination of metal and silicene superlattices allowed passing to a configuration subject to uniform periodic boundary conditions. The combination required an increase in translation vectors by 4% for aluminum and silver and 3% for gold. As shown in [29], 5% scaling of the superlattice of a composite containing silicene does not lead to any significant change in its electronic properties. The spatial translation period in the z-direction was 3 nm. The top view of the combined silicene and silver superlattices is shown in Fig. 1.

For all considered systems "silicene/substrate" geometric optimization was performed using the generalized gradient approximation in the Perdew-Burke-Ernzerhof (PBE) form [30]. In this work, a spin-orbit interaction is not taken into account. However, the adiabatic generalized gradient approximation creates an exploration opportunity for the spin-polarized the exchange-correlation interaction [31]. The buckling structure of silicene contributes to the fact that the electron spin is associated with its momentum. The strong spin-orbit interaction maintains a state with a very narrow spin-orbit gap (1.5 meV) in silicene [31,32]. This state can be

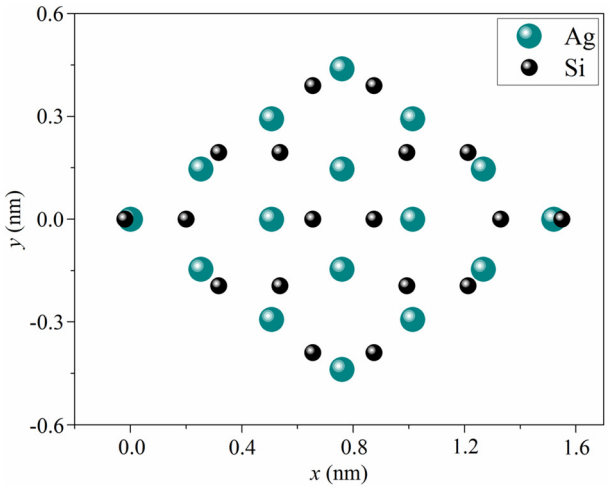

Fig. 1. Combined supercells of 4 × 4 silver and 3 × 3 silicene.

easily changed by applying a perpendicular electric field, which results in the appearance of a larger band gap in silicene.

The criterion for the end of the dynamic relaxation of atoms was the condition that the change in the total energy of the system should become less than 0.001 eV. All calculations were performed at the cutoff energy of the plane wave basis set of 500 Ry. The Brillouin zone was specified by the Monkhorst-Pack method [33] using 10 × 10 × 1 k-points. In addition, to investigate the thermal stability of the Si–Ni and Si–Cu systems, ab initio molecular dynamics calculations were performed at the temperature of 293 K. The duration of the calculations was 1000 time steps with a step length of 1 fs. The temperature in the model was maintained using a Nose thermostat [34]. The calculations were performed using the SIESTA software package [35]. The adhesion energy E_{adh} between silicene and substrates was calculated using the formula

$$E_{adh} = -\frac{E_{Tot} - E_{Si} - E_{Me}}{N_{el}}, \quad (1)$$

where E_{Tot} is the total energy of the system, E_{Si} and E_{Me} are the total energies calculated for silicene and metal (Ag, Au, Al) substrates, respectively, and N_{el} is the number of unit cells in the system.

The binding energy in the silicene sheet E^b_{Si} was determined as

$$E^b_{Si} = -\frac{E_{Tot} - E_{Me} - N_{Si}E_{1Si}}{N_{Si}}, \quad (2)$$

where E_{1Si} is the total energy calculated for one silicon atom, and N_{Si} is the number of silicon atoms in the system.

The binding energy in the metal substrate E^b_{Me} can be written as

$$E^b_{Me} = -\frac{E_{Tot} - E_{Si} - N_{Me}E_{1Me}}{N_{Me}}, \quad (3)$$

where E_{1Me} is the total energy calculated for one metal atom (Ag, Au, Al), and N_{Me} is the number of metal atoms in the system.

SIESTA software allows one to calculate the density of states (DOS) for each specified *n*- band

$$N_n(E) = \int \frac{d\mathbf{k}}{4\pi^3}\delta\big(E - E_n(\mathbf{k})\big), \quad (4)$$

where the argument $E_n(\mathbf{k})$ in the δ-function is the variance of the band, and the Brillouin zone is the region of integration. Partial spectrum (PDOS) shows which atoms in the system form certain electronic states. In addition, PDOS also discloses electron hybridization in the system.

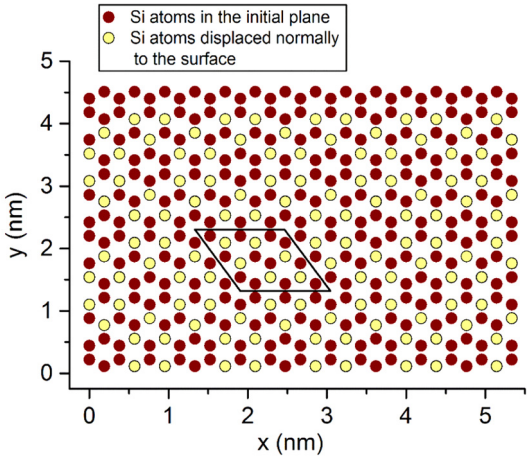

Fig. 2. Top view of the silicene structure at the initial instant; an outline shows a unit surface cell of the silicene sheet.

Table 1
Parameters of the Morse potential [21,22,42].

Interaction	D_e, eV	r_e, Å	a, Å^{-1}
Al–Si	0.4824	2.92	1.322
Ag–Si	0.2749	3.74	1.454
Au–Si	0.3286	3.68	1.561

Obviously, in silicene placed on metal substrates, mechanical stresses appear due to the non-coincidence of the lattice periods of the two materials. To calculate these stresses, it is required to increase the size of the simulated system significantly (∼100 times). Performing such calculations within the DFT model requires an extremely large amount of computer time. Therefore, this problem was solved using classical molecular dynamics.

The silicene sheet, which initial configuration is shown in Fig. 2, consists of 300 Si atoms. The unit cell, marked with a diamond in Fig. 2, contains 18 atoms. The atoms in a cell are located on two levels: 6 atoms are lifted to a height of 0.44 Å to form buckles of the same height as in the DFT model. The flower structure corresponds to that established from the experimental data for silicene on an Ag (111) substrate [36]. The distance between the lower plane of silicene and the upper layer of the substrate correspond to that determined by the ab initio calculation (0.27 nm) [37]. A silicene sheet was placed on four-layer Me (111) substrates, where Me = Al, Ag, Au. In each case, the total number of metal atoms was 1120. The substrate layers had ABAB packing and interplanar spacings, which are observed in the FCC structure of the corresponding crystals. The interaction between metal atoms in the substrate was described by the EAM potentials [38,39], and in silicene using the Tersoff potential [40]. The Me–Si cross-interaction was represented in the form of the Morse potential, which parameters are presented in Table 1. The molecular dynamics modeling was performed by parallel computations using the LAMMPS program [41].

The calculation duration was 10 million time steps. Identical to the present work, the value of the time step $\Delta t = 0.1$ fs was used in [21–23]. To calculate the stress distribution, the entire film was divided into L strips both in the direction of the $0x$ axis as well as in the direction of the $0y$ axis. The calculation of the $\sigma_{\gamma\alpha}(l)$ stress appearing in the elementary area with the number l was determined by dividing the resulting force by its S_l area. Thus, the stress state of silicene was determined using the expression

$$\sigma_{\gamma\alpha}(l) = \left\langle \sum_i^n \frac{1}{\Omega}\left(m v_\gamma^i v_\alpha^i\right)\right\rangle + \frac{1}{S_l}\left\langle \sum_i^n \sum_{j\neq i}^{(u_i\le u, u_j\ge u)} \left(f_{ij}^\alpha\right)\right\rangle, \qquad (5)$$

where n is the number of atoms on the lth area, m is the atomic mass, v_α^i is the α projection of the velocity of the ith atom, Ω is the volume per atom, f_{ij}^α is the α projection of the resulting force from the interaction between i and j atoms that passes though the lth area, and u_i is the coordinate of the atom i; the coordinate of the contact point of the straight line passing through the centers of the atoms i and j and the lth surface element is denoted through the symbol u.

A hybrid computer of the URAN cluster type at the Institute of Mathematics and Mechanics UB RAS was used for calculations.

3. Results and discussion

The energy and geometric characteristics of the silicene/metal systems calculated within the DFT model are presented in Table 2. The energy characteristics are reflected here using the adhesion energy for silicene and the metal substrate (E_{adh}) and the binding energy in the silicene sheet (E_{Si}^{b}) and in the metal substrate (E_{Me}^{b}). The geometric parameters include: average bond lengths between atoms on a metal substrate ($L_{\text{Me–Me}}$), that of silicon atoms and atoms of a metal substrate ($L_{\text{Si–Me}}$), as well as that of silicon atoms in a silicene sheet ($L_{\text{Si–Si}}$). The data labeled 3′ and 4′ correspond to substrates having a fixed z coordinate for atoms in the lower layer. Table 2 shows the effect of the thickness of the metal substrate on the binding energy and geometric properties of the systems studied. These data were obtained in the ab initio molecular dynamics calculation.

The energy of adhesion changes as the number of layers in the metal substrate increases. For example, in the silicene/aluminum system as the thickness of the aluminum substrate increases from 1 to 4, the adhesion energy decreases from 1.626 to 1.137 eV. In this case, the transition from the 4- to 5-layer aluminum substrate leads to a decrease in the adhesion energy by ∼1%. The Si–Si bond lengths determined for silicene on a five-layer aluminum substrate agree with the values obtained in [27] and are 3% less than the bond lengths calculated in [43]. In the silicene/silver systems an increase in the number of layers in the substrate from 1 to 2 causes an increase in the adhesion energy from 0.698 to 1.249 eV. The adhesion energy decreases by ∼1.6%, with a further increase in the thickness of the substrate up to 3 layers and in the case of the transition from the three-layer to four-layer substrate, the value of the adhesion energy remained unchanged. The adhesion energy between silicene and the gold substrate increases from 0.696 to 1.028 eV when the number of layers in the substrate changes from 1 to 2. A further increase in the thickness of the gold substrate from 2 to 4 layers leads to an increase in the adhesion energy by ∼2.3%. In the case of silver and gold, the thicker substrates were modeled by attaching a third (3′) fixed layer to the two-layer substrate, and then the fourth (4′) one in the case of aluminum. The obtained adhesion energies for such systems differ (by ∼1%) from the adhesion energies between silicene and five-layer metal (Al, Ag, Au) substrates. Comparison of the adhesion energies between silicene sheet and five-layer metal (Al, Ag, and Au) substrates leads to the following conclusion. The interaction between silicene and the silver substrate is expressed in the highest adhesion energy (1.241 eV), and the interaction between silicene and the gold substrate is described by the lowest one (1.046 eV).

The bond energy between silicon atoms in a silicene sheet on an aluminum substrate decreases from 5.323 to 5.284 eV as the number of substrate layers increases from 1 to 5. This indicates that the stability of the silicene sheet decreases as the number of layers in the aluminum substrate increases. An increase in the number of layers from 1 to 5 in the silver and gold substrates leads to an increase in the bond energy in the silicene sheet from 5.055 to 5.298 eV and from 5.018 to 5.122 eV, respectively. Comparison of the bond energies between silicon atoms in a silicene

Table 2
System characteristics*.

Me	N_l	E_{adh}, eV/e.c.	E^b_{Si}, eV	E^b_{Me}, eV	L_{Me-Me}, Å	L_{Si-Me}, Å	L_{Si-Si}, Å
Al	1	1.626	5.323	3.666	2.879	2.816	2.431
	2	1.424	5.262	3.696	2.889	2.818	2.400
	3	1.284	5.253	3.698	2.899	2.781	2.405
	4	1.137	5.108	3.684	2.898	2.756	2.409
	4′	1.135	5.274	3.745	2.901	2.756	2.379
	5	1.144	5.284	3.734	2.909	2.752	2.384
Ag	1	0.698	5.055	2.517	2.951	2.833	2.391
	2	1.249	5.189	2.653	2.993	2.831	2.381
	3	1.229	5.179	2.663	2.983	2.832	2.382
	3′	1.263	5.318	2.731	2.991	2.823	2.371
	4	1.256	5.210	2.682	2.943	2.886	2.381
	5	1.241	5.298	2.752	2.938	2.815	2.374
Au	1	0.696	5.018	2.395	2.973	2.889	2.367
	2	1.028	5.099	2.538	2.987	2.870	2.383
	3	1.024	5.040	2.558	3.005	2.860	2.404
	3′	1.052	5.197	2.593	2.951	2.887	2.386
	4	1.054	5.082	2.574	2.991	2.907	2.400
	5	1.046	5.122	2.605	3.022	2.893	2.398

* E_{adh} is the adhesion energy between silicene and a metal substrate; E^b_{Si} and E^b_{Me} are the average bond energies in the silicene sheet and the metal substrate, respectively; L_{Me-Me} denotes average bond lengths between atoms in a metal substrate; L_{Si-Me} denotes average bond lengths between metal and silicon atoms; L_{Si-Si} denotes average bond lengths between silicon atoms in a silicene sheet; the dash next to the N_1 value indicates that the data was obtained for a system, which lower substrate layer is fixed to z coordinates of the atoms.

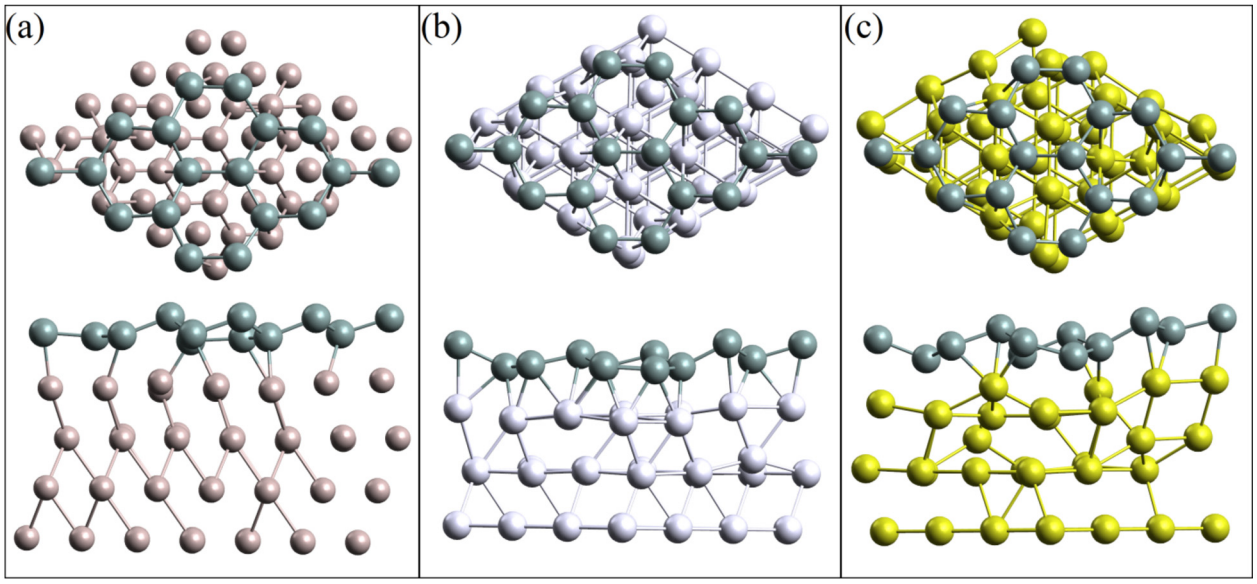

Fig. 3. Geometric structures of silicene obtained after the ab initio molecular dynamics calculation on (a) four-layer aluminum, (b) three-layer silver and (c) three-layer gold substrates with a fixed lower substrate layer.

sheet on various five-layer metal substrates (Al, Ag, Au) indicates the following. Silicene acquires the highest Si–Si bond energy on the silver substrate (5.298 eV), and the lowest one on the gold substrate (5.122 eV).

The bond lengths in metal substrates correspond to those for cubic face-centered lattices of these metals [44,45]. The average bond lengths in a silicene sheet increase from 2.28 Å, which is characteristic of an ideal freestanding silicene [46], to 2.384, 2.374, and 2.398 Å on the aluminum, silver, and gold substrates, respectively. Note that the bond lengths in silicene on a silver substrate obtained in this work are 2% longer than similar characteristics reported in [26].

Fig. 3 shows fully relaxed geometrical structures of silicene on four-layer aluminum as well as on three-layer silver and gold substrates, whose bottom layers are fixed. After the ab initio molecular dynamics calculation, the distances between the sublattices in silicene on aluminum and silver substrates increased to 0.89 and 0.82 Å, respectively. On the gold substrate, a three-level arrangement of Si atoms with distances between the levels of 0.51 and 0.75 Å was observed. These changes are associated with a separation of the first (top) layer of the substrate from the second, which is most pronounced for the gold substrate. First-principle calculations showed that the honeycomb buckled structure of silicene is not broken when it is placed on a substrate in the form of single-layer aluminum oxide (Al_2O_3) [47]. The physical properties of silicene obtained on the basis of the first-principle molecular dynamics calculations performed here are shown in Figs. 4–6.

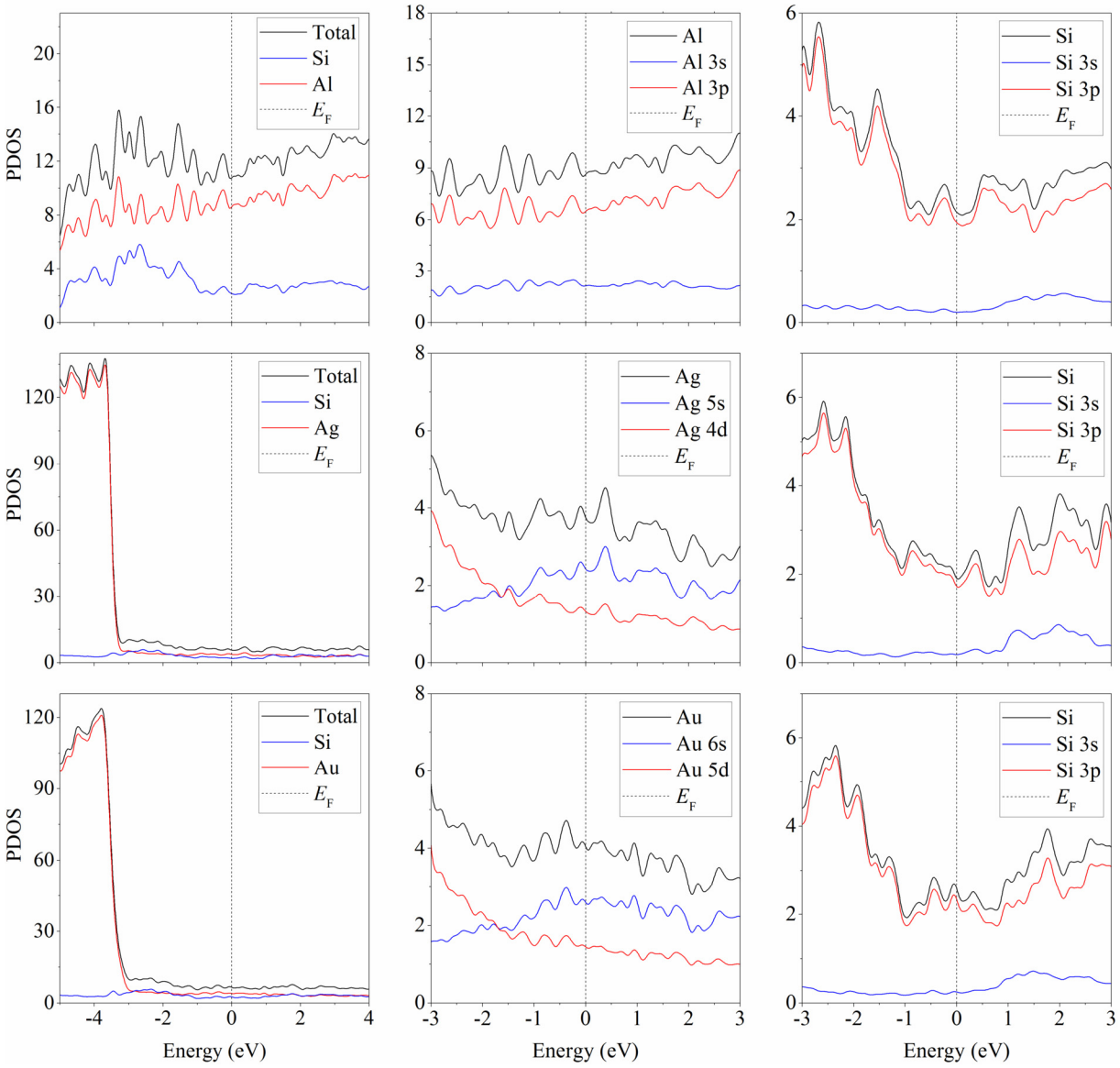

Fig. 4. Partial spectra of electronic states of the "silicene/four-layer Me substrate" system, where Me = Al, Ag, Au.

Fig. 4 shows the partial spectra of the electronic states of silicene on the four-layer aluminum, silver, and gold substrates. It is seen that silicene is metallized on the considered substrates. Thus, silicene on the aluminum substrate acquires conductive properties due to the interaction between p-electrons of silicon and aluminum; on the silver and gold substrates, the metalization occurs due to the interaction of p-electrons of silicon with s- and d-electrons of metals. The calculation of silicene PDOS placed on substrates of different thicknesses showed that, regardless of the type and thickness of the substrate, silicene acquires conductive properties.

By removing the substrate from consideration, we can determine the band structure of autonomous silicene, acquired on a substrate. Fig. 5 shows the band structures calculated for a free-standing perfect silicene in the K-Γ-M-K direction, as well as the corresponding structures for silicene after its separation from the three-layer Ag and Au substrates as well as from four-layer Al one with a lower layer fixed to z coordinates of atoms. A perfect free-standing silicene is a narrow-gap semiconductor with a straight band gap 0.033 eV [11]. Silicene separated from the aluminum substrate retains the direct band gap, which width increases to 0.294 eV. In this case, the band structure is closest to that of free-standing silicene. Note that the adsorption of Al atoms leads to a greatly enhanced buckling [9]. In addition, the data of ab initio calculations of the band gap for a one-dimensional $AlSi_3$ wire show that the value of the band gap was 0.78 eV [48]. Silicene on the gold substrate retains semiconducting properties with an indirect band gap of 0.083 eV. Whereas silicene on the silver substrate is metallized.

Normal stresses σ_{zz} are the most significant stresses that appear in silicene on the considered metal substrates. The calculated distributions of normal stresses in silicene on Al, Ag, and Au substrates are shown in Fig. 6. The stress distributions σ_{zz} in silicene on Ag and Au substrates are quite close, but nevertheless, the local stresses in this material located on the Au substrate are somewhat higher. Weaker stresses σ_{zz} in silicene on the Al substrate as compared to that on Ag and Au substrates can be explained as follows. The mass of the Al atom is 4 times less than the mass of the Ag atom and 7.3 times less than the mass of the Au atom. As a result, at the same temperature, Al atoms move much faster and vibrate with a higher frequency than Ag and Au atoms. This is especially noticeable in the surface layer in direct contact with sil-

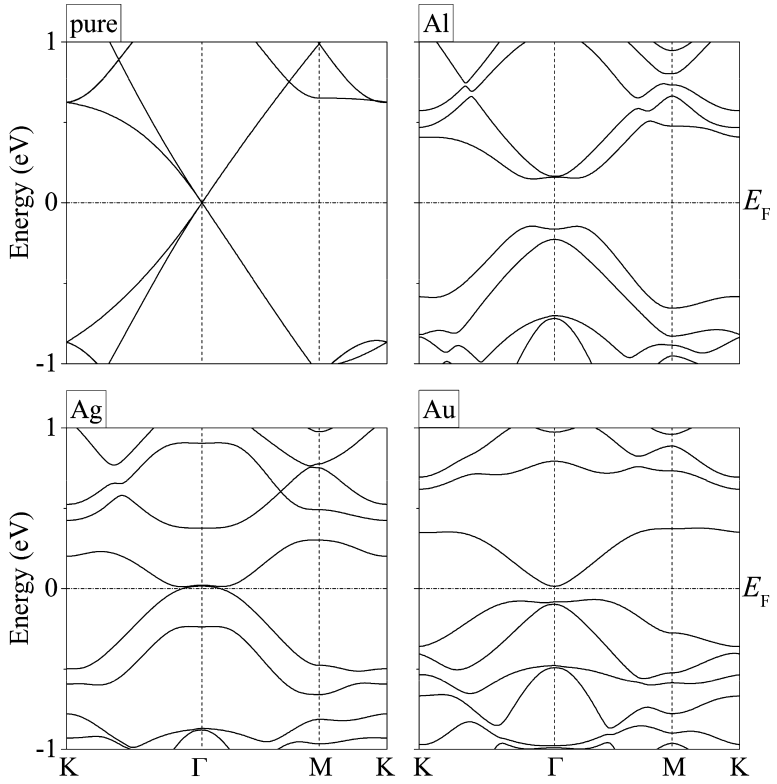

Fig. 5. Band structures in the K-Γ-M-K direction obtained from: perfect freestanding silicene and hypothetical silicene systems created by removing metal substrates: Al, Ag, and Au.

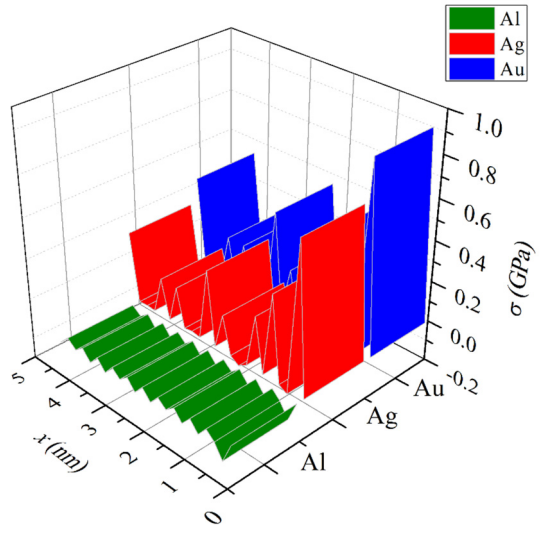

Fig. 6. Distribution of normal σ_{zz} stresses in silicene on the Al, Ag, and Au substrates along the 0x direction, when the elementary areas are elongated along the 0y direction.

icene. Therefore, the stresses formed in silicene, including normal stresses caused by contact with the substrate, rapidly dissipate on the Al substrate and remain much longer on the Ag and Au substrates. In addition, the interaction of Si atoms with an aluminum substrate is much "softer" than the interaction with Ag and Au substrates. This can be already seen by the way silicene bonds to such substrates. The energy of adhesion to the reconstructed surface of five-layer Al, Ag, and Au substrates is 0.35, 0.41, and 0.63 eV/Si atom, respectively [24].

The substantially lower and uniformly distributed normal stresses over the surface suggest the possibility of obtaining a much larger single-layer silicene on the aluminum substrate than that on the silver or gold substrates. In addition, it is easier to transfer silicene on the Al substrate to an insulating substrate by melting aluminum, since the melting point T_m of aluminum is lower than T_m of silver, gold, and silicene by a factor of 1.45, 1.61, and 1.86, respectively.

4. Conclusion

In this work, we performed a quantum mechanical modeling and classical molecular dynamics simulation of the "silicene/metal substrate" systems. The calculated spectra of electronic states indicate metalization of the "silicene/substrate" system due to the interaction of p-electrons of silicon and p-electrons of aluminum as well as p-electrons of silicon with s- and d-electrons of silver or gold. The metalization of the system is observed regardless of the thickness and type of substrate. In this case, the silicene itself, beyond the substrates, exhibits semiconductor properties with a band gap of 0.294 and 0.083 eV for configurations obtained on the aluminum and gold substrate, respectively. Whereas the silicene configuration obtained after removing the silver substrate acquires conductive properties. Calculation of the Me–Si bond energies showed that the aluminum substrate is favorable. In this case, the height of the silicene buckles depends weakly on the thickness of the substrate, remaining approximately the same as for the freestanding silicene. On the Al (111) substrate, the electronic structure of silicene has minimal distortions relative to that of autonomous silicene. However, the adhesion energy between silicene and the metal substrate is greater on the silver substrate, and it acquires lowest values on the gold substrate. From the point of view of obtaining small stresses uniformly distributed over the silicene surface, it is preferable to place silicene on the Al (111) substrate. In addition, Al is a much cheaper metal than Au and Ag. The Al element is abundant in the earth's crust. However, aluminum is easily oxidized in air with the formation of the Al_2O_3

film. Therefore, the "silicene/aluminium" 2D-material needs a protective coating preventing oxidation.

Silicene has an even better adhesion to the aluminum substrate than to the gold one, and the local stresses in silicene on the Al (111) substrate are minimal. Therefore, obtaining silicene on this cheap substrate seems to be important and relevant.

CRediT authorship contribution statement

Alexander Y. Galashev: Conceptualization, Supervision, Writing – original draft, Writing – review & editing. **Alexey S. Vorob'ev:** Formal analysis, Visualization, Writing – original draft, Writing – review & editing.

Declaration of competing interest

The authors declare that they have no known competing financial interests or personal relationships that could have appeared to influence the work reported in this paper.

References

[1] R. Mas-Balleste, C. Gomes Navarro, J. Gomez Herrero, F. Zamora, Nanoscale 3 (2011) 20, https://doi.org/10.1039/C0NR00323A.
[2] Y. Zhang, H. Li, H. Wang, R. Liu, S. Zhang, Z. Qiu, ACS Nano 9 (2015) 8514, https://doi.org/10.1021/acsnano.5b03505.
[3] M. Velicky, W.R. Hendren, W.J.I. DeBenedetti, M.A. Hines, K.S. Novoselov, H.D. Abruna, F. Huang, O. Frank, Adv. Mater. Interfaces 7 (2020) 2001324, https://doi.org/10.1002/admi.202001324.
[4] A.Y. Galashev, K.A. Ivanichkina, Lett. Mater. 9 (2019) 270, https://doi.org/10.22226/2410-3535-2019-3-270-275.
[5] B. Mortazavi, M. Shahrokhi, M.E. Madjet, T. Hussain, X. Zhuang, T. Rabczuk, J. Mater. Chem. C 7 (2019) 3025, https://doi.org/10.1039/C9TC00082H.
[6] B. Mortazavi, M. Shahrokhi, M. Makaremi, G. Cuniberti, T. Rabczuk, Mater. Today Energy 10 (2018) 336, https://doi.org/10.1016/j.mtener.2018.10.007.
[7] Y. Huang, E. Sutter, N.N. Shi, J. Zheng, T. Yang, D. Englund, H.-J. Gao, P. Sutter, ACS Nano 9 (2015) 10612, https://doi.org/10.1021/acsnano.5b04258.
[8] A.E. Galashev, Surf. Investig.: X-Ray Synchrotron Neutron Tech. 6 (2012) 623, https://doi.org/10.1134/S1027451011120056.
[9] N.T. Thuy Tran, G. Gumbs, D.K. Nguyen, M.-F. Lin, ACS Omega 5 (2020) 13760, https://doi.org/10.1021/acsomega.0c00905.
[10] S. Cahangirov, M. Topsakal, E. Aktürk, H. Sahin, S. Ciraci, Phys. Rev. Lett. 102 (2009) 236804, https://doi.org/10.1103/PhysRevLett.102.236804.
[11] A.Y. Galashev, A.S. Vorob'ev, J. Mater. Sci. 55 (2020) 11367, https://doi.org/10.1007/s10853-020-04860-8.
[12] K. Takeda, K. Shiraishi, Phys. Rev. B 50 (1994) 14916, https://doi.org/10.1103/PhysRevB.50.14916.
[13] P. Vogt, P. De Padova, C. Quaresima, J. Avila, E. Frantzeskakis, M.C. Asensio, A. Resta, B. Ealet, G. Le Lay, Phys. Rev. Lett. 108 (2012) 155501, https://doi.org/10.1103/PhysRevLett.108.155501.
[14] S. Sadeddine, H. Enriquez, A. Bendounan, P.K. Das, I. Vobornik, A. Kara, A.J. Mayne, F. Sirotti, G. Dujardin, H. Oughaddou, Sci. Rep. 7 (2017) 44400, https://doi.org/10.1038/srep44400.
[15] L. Meng, Y. Wang, L. Zhang, S. Du, R. Wu, L. Li, Y. Zhang, G. Li, H. Zhou, W.A. Hofer, H.-J. Gao, Nano Lett. 13 (2013) 685, https://doi.org/10.1021/nl304347w.
[16] M. De Crescenzi, I. Berbezier, M. Scarselli, P. Castrucci, M. Abbarchi, A. Ronda, F. Jardali, J. Park, H. Vach, ACS Nano 10 (2016) 11163, https://doi.org/10.1021/acsnano.6b06198.
[17] D. Chiappe, E. Scalise, E. Cinquanta, C. Grazianetti, B. van den Broek, M. Fanciulli, M. Houssa, Adv. Mater. 26 (2014) 2096, https://doi.org/10.1002/adma.201304783.
[18] C. Grazianetti, S. de Rosa, C. Martella, P. Targa, D. Codegoni, P. Gori, O. Pulci, A. Molle, S. Lupi, Nano Lett. 18 (2018) 7124, https://doi.org/10.1021/acs.nanolett.8b03169.
[19] A. Fleurence, R. Friedlein, T. Ozaki, H. Kawai, Y. Wang, Y. Yamada-Takamura, Phys. Rev. Lett. 108 (2012) 245501, https://doi.org/10.1103/PhysRevLett.108.245501.
[20] R. Quhe, Y. Yuan, J. Zheng, Y. Wang, Z. Ni, J. Shi, D. Yu, J. Yang, J. Lu, Sci. Rep. 4 (2014) 5476, https://doi.org/10.1038/srep05476.
[21] A.Y. Galashev, K.A. Ivanichkina, J. Electrochem. Soc. 165 (2018) A1788, https://doi.org/10.1149/2.0751809jes.
[22] A.Y. Galashev, K.A. Ivanichkina, Electrochemistry 6 (2019) 1525, https://doi.org/10.1002/celc.201900119.
[23] A.Y. Galashev, K.A. Ivanichkina, K.P. Katin, M.M. Maslov, ACS Omega 5 (2020) 13207, https://doi.org/10.1021/acsomega.0c01240.
[24] Z. Majzik, M.R. Tchalala, M. Švec, P. Hapala, H. Enriquez, A. Kara, A.J. Mayne, G. Dujardin, P. Jelínek, H. Oughaddou, J. Phys. Condens. Matter 25 (2013) 225301, https://doi.org/10.1088/0953-8984/25/22/225301.
[25] Y.-P. Wang, H.i-P. Cheng, Phys. Rev. B 87 (2013) 245430, https://doi.org/10.1103/PhysRevB.87.245430.
[26] Z.-X. Guo, S. Furuya, J.-I. Iwata, A. Oshiyama, Phys. Rev. B 87 (2013) 235435, https://doi.org/10.1103/PhysRevB.87.235435.
[27] T. Morishita, M.J.S. Spencer, S. Kawamoto, I.K. Snook, J. Phys. Chem. C 117 (2013) 22142, https://doi.org/10.1021/jp4080898.
[28] J.M. Soler, E. Artacho, J.D. Gale, A. García, J. Junquera, P. Ordejon, D. Sanchez-Portal, J. Phys. Condens. Matter 14 (2002) 2745, https://doi.org/10.1088/0953-8984/14/11/302.
[29] W. Hu, Z. Li, J. Yang, J. Chem. Phys. 139 (2013) 154704, https://doi.org/10.1063/1.4824887.
[30] J.P. Perdew, K. Burke, M. Ernzerhof, Phys. Rev. Lett. 77 (1996) 3865, https://doi.org/10.1103/PhysRevLett.77.3865.
[31] C.C. Liu, W. Feng, Y. Yao, Phys. Rev. Lett. 107 (2011) 076802, https://doi.org/10.1103/PhysRevLett.107.076802.
[32] N.D. Drummond, V. Zólyomi, V.I. Fal'ko, Phys. Rev. B 85 (2012) 075423, https://doi.org/10.1103/PhysRevB.85.075423.
[33] H.J. Monkhorst, J.D. Pack, Phys. Rev. B 13 (1976) 5188, https://doi.org/10.1103/PhysRevB.13.5188.
[34] S. Nose, J. Chem. Phys. 81 (1984) 511, https://doi.org/10.1063/1.447334.
[35] D. Sanchez-Portal, P. Ordejon, E. Artacho, J.M. Soler, Int. J. Quant. Chem. 65 (1997) 453, https://doi.org/10.1002/(SICI)1097-461X(1997)65:5<453::AID-QUA9>3.0.CO;2-V.
[36] R.K. Bhavadharani, V. Nagarajan, R. Chandiramouli, Condens. Matter Phys. 22 (2019) 33001, https://doi.org/10.5488/CMP.22.33001.
[37] A.E. Galashev, K.A. Ivanichkina, O.R. Rakhmanova, Yu.P. Zaikov, Lett. Mater. 8 (2018) 463, https://doi.org/10.22226/2410-3535-2018-4-463-467.
[38] S.M. Foiles, M.I. Baskes, M.S. Daw, Phys. Rev. B 33 (1986) 7983, https://doi.org/10.1103/PhysRevB.33.7983.
[39] Y. Mishin, D. Farkas, M.J. Mehl, Phys. Rev. B 59 (1999) 3393, https://doi.org/10.1103/PhysRevB.59.3393.
[40] J. Tersoff, Phys. Rev. B, Condens. Matter Mater. Phys. 39 (1989) 5566, https://doi.org/10.1103/PhysRevB.39.5566.
[41] S. Plimpton, J. Comput. Phys. 117 (1995) 1, https://doi.org/10.1006/jcph.1995.1039.
[42] J.K. Singh, J. Adhikari, S. Kyu Kwak, Fluid Phase Equilib. 248 (2006) 1, https://doi.org/10.1016/j.fluid.2006.07.010.
[43] Y. Sato, Y. Fukaya, M. Cameau, A.K. Kundu, D. Shiga, R. Yukawa, K. Horiba, C.-H. Chen, A. Huang, H.-T. Jeng, T. Ozaki, H. Kumigashira, M. Niibe, I. Matsuda, Phys. Rev. Mater. 4 (2020) 064005, https://doi.org/10.1103/PhysRevMaterials.4.064005.
[44] F.C. Maier, S. Hocker, S. Schmauder, M. Fyta, J. Alloys Compd. 777 (2019) 619, https://doi.org/10.1016/j.jallcom.2018.10.340.
[45] V.A. Lubarda, Mech. Mater. 35 (2003) 53, https://doi.org/10.1016/S0167-6636(02)00196-5.
[46] J. Zhuang, X. Xu, H. Feng, Z. Li, X. Wang, Y. Du, Sci. Bull. 60 (2015) 1551, https://doi.org/10.1007/s11434-015-0880-2.
[47] P. Gori, I. Kupchak, F. Bechstedt, D. Grassano, O. Pulci, Phys. Rev. B 100 (2019) 245413, https://doi.org/10.1103/PhysRevB.100.245413.
[48] M.W. Chuan, K.L. Wong, A. Hamzah, S. Rusli, N.E. Alias, C.S. Lim, M.L.P. Tan, Physica E, Low-Dimens. Syst. Nanostruct. 116 (2020) 113731, https://doi.org/10.1016/j.physe.2019.113731.